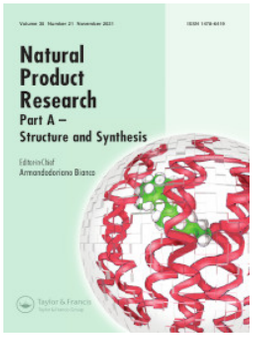

Taylor & Francis
Taylor & Francis Group

Natural Product Research

Formerly Natural Product Letters

ISSN: (Print) (Online) Journal homepage: https://www.tandfonline.com/loi/gnpl20

The 2,3-epoxy naphthoquinol produced by endophyte *Arthrinium marii* M-211

Ferry Ferdiansyah Sofian, Takuma Suzuki, Unang Supratman, Desi Harneti, Rani Maharani, Supriatno Salam, Fajar Fauzi Abdullah, Jun Yoshida, Yoshiaki Ito, Takuya Koseki & Yoshihito Shiono

To cite this article: Ferry Ferdiansyah Sofian, Takuma Suzuki, Unang Supratman, Desi Harneti, Rani Maharani, Supriatno Salam, Fajar Fauzi Abdullah, Jun Yoshida, Yoshiaki Ito, Takuya Koseki & Yoshihito Shiono (2021): The 2,3-epoxy naphthoquinol produced by endophyte *Arthrinium marii* M-211, Natural Product Research, DOI: 10.1080/14786419.2021.1998899

To link to this article: https://doi.org/10.1080/14786419.2021.1998899

NATURAL PRODUCT RESEARCH
https://doi.org/10.1080/14786419.2021.1998899

The 2,3-epoxy naphthoquinol produced by endophyte *Arthrinium marii* M-211

Ferry Ferdiansyah Sofian[a,b], Takuma Suzuki[a], Unang Supratman[c], Desi Harneti[c], Rani Maharani[c], Supriatno Salam[c,d], Fajar Fauzi Abdullah[e], Jun Yoshida[f], Yoshiaki Ito[g], Takuya Koseki[a] and Yoshihito Shiono[a,b]

[a]Department of Food, Life, and Environmental Science, Faculty of Agriculture, Yamagata University, Tsuruoka, Yamagata, Japan; [b]The United Graduate School of Agricultural Sciences, Iwate University, Morioka, Iwate, Japan; [c]Department of Chemistry, Faculty of Mathematics and Natural Sciences, Universitas Padjadjaran, Jatinangor, Sumedang, Indonesia; [d]Faculty of Pharmacy, Universitas Mulawarman, Samarinda, Kalimantan Timur, Indonesia; [e]Department of Chemistry, Faculty of Mathematics and Natural Sciences, Universitas Garut, Garut, Indonesia; [f]Center for Liberal Arts and Sciences, Iwate Medical University, Yahaba, Iwate, Japan; [g]Department of Biological Chemistry and Food Science, Faculty of Agriculture, Iwate University, Morioka, Iwate, Japan

ABSTRACT

A novel 2,3-epoxy naphthoquinol, named (6*R*,7*R*,8*R*)-theissenone A (**1**), possessing an oxatricyclo[5.4.0.0^{3,5}]undeca-trien-2-one skeleton, together with two known compounds, (6*S*,7*R*,8*R*)-theissenone (**2**) and arthrinone (**3**), were produced by an endophytic fungus, *Arthrinium marii* M-211, which was isolated from mangrove plants. The structure of **1**, including the absolute stereochemistry, was elucidated by analysis of nuclear magnetic resonance (NMR) and mass spectrometry (MS) data and time-dependent density functional theory (TDDFT) calculations of electronic circular dichroism (ECD) spectra. Additionally, the absolute structure of **2** was deduced as a diastereomer of **1** using ECD spectral data analysis. Compounds **1**, **2** and **3** exhibited cytotoxic activity against the H4IIE rat hepatoma cells, with IC_{50} values of 67.5, 46.6 and 13.4 μM, respectively.

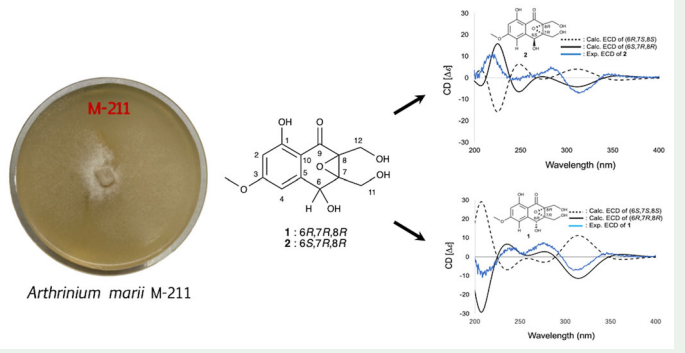

ARTICLE HISTORY
Received 22 June 2021
Accepted 13 October 2021

KEYWORDS
Theissenone A; OSMAC; cytotoxicity; H4IIE hepatoma cell line

CONTACT Yoshihito Shiono yshiono@tds1.tr.yamagata-u.ac.jp Department of Food, Life, and Environmental Science, Faculty of Agriculture, Yamagata University, Tsuruoka, Yamagata 997-8555, Japan.

Supplemental data for this article can be accessed online at https://doi.org/10.1080/14786419.2021.1998899.

1. Introduction

Fungal secondary metabolites possess unique chemical structures and are widely considered to be one of the best repositories for drug discovery from natural sources, due to their extensive biological activities. However, increasing evidence from fungal genetic studies has shown that many biosynthesis genes responsible for the production of fungal secondary metabolites are not expressed or are downregulated under standard laboratory conditions. Therefore, this biosynthetic potential is not being effectively exploited. A genome includes silent genes clusters that are inactive under normal environmental conditions. Several strategies have been revealed that can activate these silent gene clusters and gain access to this untapped reservoir of potentially bioactive compounds. In recent years, some researchers have demonstrated that an OSMAC ('one strain many compounds') strategy could induce the production of new secondary metabolites (Bode et al. 2002). OSMAC strategies are aimed at triggering potential or silent gene clusters in microorganisms (Frank et al. 2019).

Previously, we used the OSMAC approach to obtain the vertinolide derivatives produced by the endophytic fungus *Clonostachys rosea* B5-2, isolated from a branch of *Bruguiera gymnorrhiza* (L.) Lamk., simply by cultivating the fungus in media containing fruit juice, such as apple juice (Supratman et al. 2019). The results of this work encouraged us to investigate further the effects of apple juice in endophytic fungi, with the aiming of producing new metabolites. During our programme of isolating endophytes for their chemical diversity, and screening using drug discovery paradigms, we encountered an endophyte, characterised as *Arthrinium marii* M-211. This was isolated from the mangrove species *Bruguiera gymnorrhiza* (L.) Lamk., which was growing in Santolo Garut Beach, West Java, Indonesia. Cultivation of this M-211 fungus strain in media containing apple juice led to the production of a new 2,3-epoxy naphthoquinol, named theissenone A (**1**), together with two known compounds, theissenone (**2**) (Hsieh et al. 2021) and arthrinone (**3**) (Qian-Cutrone et al. 1994) (Figure 1). Herein, we report the isolation and characterisation of a new metabolite, **1**, from the endophytic fungus *A. marii* M-211, which was cultivated in apple juice-containing rice media. As an additional supporting data, we deduce the absolute stereochemistry of **2** using the comparison of calculated and experimental ECD data of **2**, which was not conducted in the previous literature report.

2. Results and discussions

Theissenone A (**1**) was isolated as a white powder. It had the molecular formula $C_{13}H_{14}O_7$ (seven double-bond equivalents), based on high-resolution electrospray

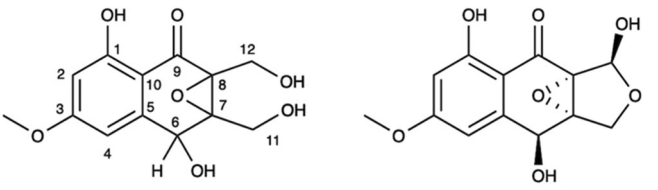

1 : 6*R*,7*R*,8*R*
2 : 6*S*,7*R*,8*R*

3

Figure 1. Structures of **1**, **2** and **3**.

ionization time-of-flight mass spectrometry (HRESITOFMS) analysis (Supplementary Figure S13), indicating seven degrees of unsaturation. The infrared (IR) spectrum displayed absorptions attributable to hydroxyl (3334 cm^{-1}), conjugated keto carbonyl (1630 cm^{-1}), and phenol (1340 cm^{-1}) functionalities. The ultraviolet (UV) spectrum showed two absorption maximums at 291 and 330 nm, which suggested the presence of an aromatic carbonyl chromophore with possible *ortho/para* substitution by a hydroxyl group on the aromatic ring (Qian-Cutrone et al. 1994). The ^{1}H nuclear magnetic resonance (NMR) data (Supplementary Table S1) of **1** exhibited signals for one methoxy group at δ_H 3.87 (s, 3-OMe), two oxymethylene groups at δ_H 3.78 (1H, d, $J = 12.0$ Hz, Ha-11) and 4.55 (1H, d, $J = 12.0$ Hz, Hb-11) and 3.72 (1H, d, $J = 12.0$ Hz, Ha-12) and 4.71 (1H, d, $J = 12.0$ Hz, Hb-12), one oxymethine group at δ_H 5.28 (1H, d, $J = 8.4$ Hz, H-6), and two meta-coupled aromatic protons at δ_H 6.39 (1H, d, $J = 2.0$ Hz, H-2) and 6.84 (1H, d, $J = 2.0$ Hz, H-4). Interpretation of the ^{13}C NMR (Supplementary Table S1) and distortionless enhancement by polarization transfer (DEPT) data (Supplementary Figure S5) revealed thirteen carbon signals attributable to one methoxyl, with resonances at δ_C 55.4; two sp^3 quaternary carbons at δ_C 57.0 and 65.0, suggesting the presence of a fully substituted epoxy group; two oxymethylenes at δ_C 60.2 and 66.7; one oxymethine at δ_C 63.9; six aromatic signals at δ_C 99.7, 106.9, 145.5, 106.9, 165.1 and 167.1, implying the presence of a 1,2,3,5-subtituted benzene ring; and one carbonyl at δ_C 196.4. In addition, by detailed analyses of the ^{1}H NMR (Supplementary Figure S1) and heteronuclear multiple quantum coherence (HMQC) spectra (Supplementary Figure S6), one hydroxy proton at δ_H 5.39 and one phenolic hydroxy proton involved in hydrogen bonding at δ_H 12.0 were identified in the downfield region of the ^{1}H NMR spectrum. These aforementioned spectroscopic data demonstrated six degrees of unsaturation, so that one remaining additional ring should be attributed in the molecule.

Further analysis of the heteronuclear multiple bond coherence (HMBC) correlations (Supplementary Figure S12), from H-2 to C- 4 and C-10; from H-4 to C-2, C-6 and C-10; and from H-6 to C-8 and C-10, resulted in the elucidation of a 2,3-epoxy naphthoquinol moiety. In addition, the HMBC correlations from H-11 to C-6 and C-8 and from H-12 to C-7 and C-9, indicated methylenes of H-11 and H-12 were connected to C-7 and C-8, respectively (Supplementary Figure S12). The absolute configuration of **1** was elucidated by comparison between the calculated electronic circular dichroism (ECD) data at the B3LYP/6–311 G (d) level with the conductor-like polarizable continuum model (CPCM) in MeOH solution and the experimental ECD spectrum (Supplementary Figure S15). The experimental ECD curve of **1** matched well with the computer-simulation ECD of 6*R*,7*R*,8*R*. Therefore, the stereostructure of **1** was established as shown (Figure 1).

Compounds **2** and **3** were determined to be theissenone (Hsieh et al. 2021) and arthrinone (Qian-Cutrone et al. 1994), respectively. A detailed comparison of the chemical shifts and coupling constants between the ^{1}H NMR spectra of **1** and **2** in acetone-d_6 revealed several differences in the signals of the methine proton (H-4, H-6 and H-11) and the hydroxyl proton (6-OH) (Supplementary Table S1). The obvious differences consisted of the inversion of the chemical shifts of H-4, H-11 and 6-OH. These differences suggest that **2** is the diastereomer of **1**, which showed the different configuration

at C-6. According to the literature report (Hsieh et al. 2021), **2** was proposed to be originated from **3**, suggesting that the absolute configuration of **2** was determined as 6*S*,7*R*,8*R*. In this experiment, we tried to deduce the absolute stereochemistry of **2** using ECD spectral data analysis for supporting data information. Consequently, the absolute configuration of **2** was confirmed as 6*S*,7*R*,8*R* by a comparison of the experimental and calculated ECD spectra (Supplementary Figure S15), as the same result as the literature.

To know the biocompatibility of the isolated compounds, all three compounds (**1**–**3**) were evaluated for cytotoxic activities against H4IIE hepatoma cells, using an MTT assay (Yoshida et al. 2017). Compounds **2** and **3** showed cytotoxic activity, with IC_{50} values of 46.6 and 13.4 μM, respectively, while the positive control staurosporine exhibited an $IC_{50} = 20.9$ nM. Compound **1** was not cytotoxic at low concentrations, but suppresses cell viability at 67.5 μM (50–200 μM) (Supplementary Figure S22 and Table S4). In addition, compounds **1**–**3** showed moderate antimicrobial activity against both *Pseudomonas aeruginosa* ATCC 15442 [Minimum Inhibitory Concentration (MIC) values (μg/mL): **1**, 25; **2**, 25; **3**, 12.5] and *Staphylococcus aureus* NBRC 13276 [MIC values (μg/mL): **1**, 25; **2**, 25; **3**, 12.5] (Supplementary Table S5), using an agar dilution method (Shiono et al. 2005). Otherwise, none of compounds **1**–**3** showed antimicrobial activity against both *Aspergillus clavatus* F 318a and *Candida albicans* ATCC 2019 (Table S5). The results of this biological study suggest that the epoxynaphtho[2,3-c]furan ring moiety is associated with more cytotoxic activity compared with that of 2,3-epoxy naphthoquinol moieties of **1** and **2**. Moreover, the configuration of 6*S* in between the benzene ring and the epoxynaphtho[2,3-c]furan ring is affecting the cytotoxic properties. The higher cytotoxicity of **3** compared with that of **1** and **2** was attributed to its increased hydrophobicity, making it easier for it to cross the cell membrane. Our findings suggest that compound **3** could be a potential candidate for further investigations into the molecular mechanism of the action on targets of cytotoxicity.

3. Experimental

3.1. General experimental procedures

Optical rotation was measured using a Horiba SEPA-300 polarimeter (*Horiba*, Japan). IR and UV-vis spectra were respectively recorded with Horiba FT710 (*Horiba*, Japan) and Shimadzu UV-1800 spectrometer (*Shimadzu*, Japan). Mass spectra was obtained with a Synapt G2 (*Water Corporation*, USA) and JEOL HX110 mass spectrometer (*JEOL*, Japan). NMR data were recorded on JEOL ECZ-600 spectrometer (*JEOL,* Japan) at 600 MHz for ^{1}H and 150 MHz for ^{13}C. Chemical shift is given on a δ (ppm) scale with TMS as an internal standard. ^{1}H, ^{13}C, DEPT, COSY, HMQC and HMBC spectra were recorded using standard JEOL pulse sequences. Column chromatography were conducted on silica gel 60 (*Kanto Chemical Co.*, Inc., Japan) and ODS (*Fuji Silysia*, Japan). Flash chromatography was conducted using Büchi Flash Chromatography C-601 (*Büchi,* Switzerland) and packed column Biotage® SNAP Ultra (*Biotage*, Sweden) 10 g (25 μm). HPLC separations were carried out using Shimadzu LC-20AT and UV-vis detector SPD-20A (*Shimadzu,* Japan) on reverse phase-high performance liquid chromatography (RP-HPLC) packed

column C_{18} column (Cosmosil 5 C_{18}-MS, 5 μm, 6.0 mm I.D. × 250 mm) (Nacalai tesque, Inc. Kyoto, Japan). Thin layer chromatography (TLC) was carried out on precoated silica gel 60 F_{254} plates (*Merck*, Germany) and spot were detected by spraying with 1% vanillin in H_2SO_4 followed by heating or by UV irradiation.

3.2. Fungal material, fermentation and isolation

The fungal strain M-211 was isolated from inner tissue of dead branch collected in the Santolo beach area (southern latitude 7°65′00″, east longitude 107°68′76″), Garut, West Java, Indonesia. This strain was identified as *Arthrinium marii* using DNA analysis of the 18S rRNA regions with GenBank Accession No. LC644660. The voucher specimen of this fungus (code number M-211) was deposited at our laboratory in the Faculty of Agriculture, Yamagata University.

A. marii M-211 was cultivated on sterilized brown rice (120 g in five 1 L flasks) at 25 °C for four weeks. M-211 strain was cultured on slants with PDA at 28°C for 5 days. Fermentation was carried out in Erlenmeyer flasks (1000 mL) containing 50 g of rice and apple juice (70 mL per flask; total of 2300 g). After autoclaving, each flask was inoculated with hyphae inoculum and incubated at 25°C for one month. The mycelia and solid rice medium were extracted with MeOH, then the extract was concentrated under reduced pressure to give a crude extract and the suspended in distilled water. The resulting aqueous concentrate was partitioned into EtOAc layer and then concentrated under reduced pressure to give a crude extract of EtOAc (3.5 g). The extract was separated by silica gel column chromatography with a stepwise elution of *n*-hexane/EtOAc (100:0–0:100, *v/v*; each 500 ml) to give 11 fractions (Frs. 1-1 to 11). Frs. 1-6 and 1-7 (50–60% *n*-Hexane/EtOAc, 1.0 g) were combined and further separated on a silica gel column with $CHCl_3$/EtOAc to provide 11 fractions (Frs. 2-1 to 11). Fr. 2-5 was separated by flash chromatography with an elution using $CHCl_3$ containing 40% EtOAc to give 11 fractions (Frs. 3-1 to 11). Fr. 3-6 (400 mg) was subjected to ODS column chromatography by eluting stepwise with 100% H_2O to 100% MeOH (100:0–0:100, *v/v*; each 50 ml), which yielded 11 fractions (Frs. 3-6-1 to 11). Fr. 3-6-4 (31 mg) was subjected to flash silica gel CC ($CHCl_3$/MeOH, 50:1, *v/v*) to afford arthrinone (**3**, 17.0 mg). Fr. 3-6-5 (55.0 mg) was purified by semipreparative HPLC using a Cosmosil 5 C_{18}-MS packed column (5 μm, 6.0 mm I.D. × 250 mm) at a flow rate of 1.0 mL/min (H_2O–MeOH, 30:70) to afford (6*S*,7*R*,8*R*)-theissenone (**2**, 15.0 mg, t_R = 5.2 min) and (6*R*,7*R*,8*R*)-theissenone A (**1**, 8.0 mg, t_R = 5.5 min).

(*6R,7R,8R*) *-theissenone A (1)*. White amorphous powder; $[\alpha]_D^{25}$ +66 (*c* 0.62, MeOH); UV(MeOH) λ_{max} (log ε) nm: 218 (4.7), 238 (4.5), 290 (4.7), 323 (4.5) nm; IR (KBr) ν_{max} 3334, 2927, 1630, 1340, 1295, 1208, 1150 cm^{-1}; CD (MeOH) λ_{max} ($\Delta\varepsilon$) 208 (−10), 240 (5.6), 275 (6.7), 312 (-7.1) nm; ^{1}H-NMR (600 MHz, acetone-d_6) δ_H 12.0 (1H, s, 1-OH), 6.84 (1H, d, *J* = 2.0 Hz, H-4), 6.39 (1H, d, *J* = 2.0 Hz, H-2), 5.39 (1H, br. d, *J* = 8.4 Hz, 6-OH), 5.28 (1H, d, *J* = 8.4 Hz, H-6), 4.71 (1H, d, *J* = 12.0 Hz, H-12b), 4.55 (1H, d, *J* = 12.0 Hz, H-11b), 3.87 (3H, s, 3-OMe), 3.78 (1H, d, *J* = 12.0 Hz, H-11a), 3.72 (1H, d, *J* = 12.0 Hz, H-12a); ^{13}C-NMR (150 MHz, acetone-d_6) δ_C 196.4 (C-9), 167.1 (C-3), 165.1 (C-1), 145.5 (C-5), 106.9 (C-4), 106.9 (C-10), 99.7 (C-2), 66.7 (C-11), 65.0 (C-8), 63.9 (C-6), 60.2 (C-12), 57.0

(C-7), 55.4 (3-OMe); HRESITOFMS *m/z* 305.0638 ($[M + Na]^+$, calcd. for $C_{13}H_{14}O_7Na$, 305.0637).

3.3. ECD calculations

In order to clarify the absolute configuration of **1** and **2**, computational methods were utilized. The DFT and TDDFT calculations were carried out in the gas phase with Gaussian 09 software (Frisch et al. 2010). Conformational analyses of **1** and **2** have been realized using the GMMX package and the MMFF94 force field with a 3.5 kcal/mol energy threshold. Conformers were obtained for (6*R*,7*S*,8*S*), (6*S*,7*S*,8*S*), (6*S*,7*R*,8*R*) and (6*R*,7*R*,8*R*). The conformers were further optimized with the software package Gaussian 09 at the B3LYP/6-31G (d) level, and the harmonic vibrational frequencies were also calculated to confirm their stability. The stable conformers were subjected to ECD calculation by time-dependent density functional theory (TD-DFT) method at the B3LYP/6-311G (d) level in MeOH. The ECD spectra of different conformers were simulated using a Gaussian function with a half-band width of 0.36 eV, and the final ECD spectra were obtained according to the Boltzmann distribution of each conformer. The calculated ECD spectra were compared with the experimental ones.

3.4. Evaluation for cytotoxic activity against H4IIE cells

3.4.1. Cell culture

H4IIE cells (American Type Culture Collection [ATCC], Manassas, VA, USA) were grown to sub-confluence in DMEM supplemented with 10% heat-inactivated fetal bovine serum and penicillin-streptomycin at 37 °C under a 5% CO_2 atmosphere in a humidified incubator (Yoshida et al. 2017).

3.4.2. Cell viability assay

Cell viability was determined using the MTT assay. Briefly, H4IIE cells were seeded at 2×10^4 cells/well in a 96-well plate and were treated with test sample. After 48 h, 10 μL of MTT solution (5 mg/ml in PBS) was added and the mixture was incubated at 37 °C for 4 h. At the end of the incubation period, the resultant formazan crystals were dissolved in 0.04 M HCl/isopropanol (100 μL) and the absorbance intensity was measured by using a microplate reader (Multiskan GO Microplate Spectrophotometer, Thermo Fisher Scientific) at 560 nm. The average of three independent experiments was used to calculate results from each concentration to generate half maximal inhibitory concentration (IC_{50}) values and estimate the surviving fraction of cells.

3.4.3. Statistical analysis

Data are presented as mean ± standard deviation (SD). One-way ANOVA followed by the Dunnett test was used. $p < 0.01$ and $p < 0.05$ indicated statistical significance.

3.5. Antimicrobial assay

The antimicrobial activity was determined by the paper disk diffusion method (100 μg compound in 8 mm paper disk), using meat peptone agar for *Pseudomonas aeruginosa* ATCC 15442 and *Staphylococcus aureus* NBRC 13276, potato dextrose agar for *Aspergillus clavatus* F 318a and peptone yeast agar for *Candida albicans* ATCC 2019. Compounds which showed significant inhibition zone were apply to further experiment to determine the minimal inhibitory concentration (MIC). MIC is defined as the lowest concentration resulting in no visible growth after incubation. The MIC was determined by the agar dilution based on reported reference with slight modification (Shiono et al. 2005). Chloramphenicol was used for positive control against *S. aureus* and *P. aeruginosa* (each 1 μg/mL), respectively.

Acknowledgements

The authors thank Prof. Hiroyuki Konno and Prof. Takako Aboshi in Yamagata University for CD and MS experimental supports, respectively.

Disclosure statement

The authors declare that they have no conflict of interest.

Funding

This work was partly supported by MEXT KAKENHI Grant Number 19K05709 (Y. S) and the author (U. S) was also supported by World Class Professor Grant Number T/83/D2.3/KK.04.05/2019, Indonesia.

References

Bode HB, Bethe B, Höfs R, Zeeck A. 2002. Big effects from small changes: possible ways to explore nature's chemical diversity. ChemBioChem. 3(7):619–627.

Frank M, Can Özkaya F, Müller WEG, Hamacher A, Kassack MU, Lin W, Liu Z, Proksch P. 2019. Cryptic secondary metabolites from the sponge-associated fungus *Aspergillus ochraceus*. Mar Drugs. 17(2):1–13.

Frisch MJ, Trucks GW, Schlegel HB, Scuseria GE, Robb MA, Cheeseman JR, Scalmani G, Barone V, Mennucci B, Petersson GA, et al. 2010. Gaussian 09. Revision A.02. Wallingford (CT): Gaussian, Inc.

Hsieh MH, Hsiao G, Chang CH, Yang YL, Ju YM, Kuo YH, Lee TH. 2021. Polyketides with anti-neuroinflammatory activity from *Theissenia cinerea*. J Nat Prod. 84(7):1898–1903.

Qian-Cutrone J, Gao Q, Huang S, Klohr SE, Veitch JA, Shu Y-Z. 1994. Arthrinone, a novel fungal metabolite from *Arthinium* sp. FA 1744. J Nat Prod. 57(12):1656–1660.

Shiono Y, Murayama T, Takahashi K, Okada K, Katohda S, Ikeda M. 2005. Three oxygenated cyclohexenone derivatives produced by an endophytic fungus. Biosci Biotechnol Biochem. 69(2):287–292.

Supratman U, Suzuki T, Nakamura T, Yokoyama Y, Harneti D, Maharani R, Salam S, Abdullah FF, Koseki T, Shiono Y. 2019. New metabolites produced by endophyte *Clonostachys rosea* B5 − 2. Nat Prod Res. 35:1525–1531.

Yoshida J, Uesugi S, Kawamura T, Kimura K, Hu D, Xia S, Toyooka N, Ohnishi M, Kawashima H. 2017. (4*Z*,15*Z*)-Octadecadienoic acid inhibits glycogen synthase kinase-3β and glucose production in H4IIE cells. Lipids. 52(3):295–301.